Unnamed Article

ristoke[a]

[a]*Affiliation not available*

A Review of the Behaviour of Fuel Drops in a Fuel Spray in the Context of Biofuels

Riho Kägo, Risto Ilves*, Arne Küüt, Jüri Olt

Estonian University of Life Sciences, Institute of Technology, Kreutzwaldi 56, Tartu, 51006, Estonia

Abstract: In addition to gasoline and diesel fuel, the biofuels HVO and FAME have been taken into wide use during the last decades. The properties of gasoline and diesel fuel and their effect on the combustion process have been studied for a long time, however, HVO and FAME are still being studied. Existing studies show that the use of biodiesels reduces the level of several exhaust gas emissions (like soot) in engine exhaust gases. At the same time, the reasons for the reduction of emission compounds remain unclear. The reason for determining of the drop's size and behavior is the assessment of the quality of air-fuel mixture in order to explain the reduction of soot emission in the use of biodiesels. The aim of this review paper is to provide an overview of the behavior of fuel drop and their size in fuel injectors when using different biofuels by giving a theoretical background based on literature, on the basis of which the calculations give an opportunity to evaluate experimental results of the behavior of different biofuels in the fuel spray. This study compares four different fuel types according to the WAVE-RT model. In addition, the collision mechanisms of drops (reflexive and stretching separation) are presented and these shall be compared for the fuel types. The results show that during the use of biofuels, the drop size is somewhat larger compared to diesel fuel.

Keywords: biodiesel, fuel drop size, FAME, HVO, diesel engine

1. Introduction

The use of biofuels is growing in the world. The EU directive prescribes that by the year 2020 10% of the energy used in the transport sector must be constituted by biofuels [1]. The Paris Agreement aims to increase further the share of biofuels in the transport sector. Several studies have been performed on the use of biofuels in internal combustion engines. The main focus has been on the effects of biofuels on engine 's exhaust gases, work surfaces, fuel preservation, blending with fossil fuels etc. The results show that when, for example, biodiesel (for example, FAME or RME) is used as engine fuel, then the level of soot decreases in exhaust gases. At this point, the decrease of the level of soot in exhaust gases is explained by more efficient combustion as biodiesel contains oxygen [2, 3, 4, 5, 6, 7, 8, 9, 10, 11, 12, 13, 14, 15, 16, 17, 18, 19, 20, 21, 22, 23, 24, 25, 26, 27, 28, 29, 30, 31, 32, 33, 34, 35, 36, 37, 38, 39, 40, 41, 42, 43, 44, 45, 46, 47, 48, 49, 50, 51, 52, 53, 54, 55, 56, 57, 58].

At the same time, when HVO is used, the level of soot in engine exhaust gas is also reduced [59, 60]. Therefore, the oxygen content in the fuel cannot be used as the actual reason for explaining the reduction of the level of soot.

In order to provide a better overview, a theoretical analysis of the injection of biofuels into engine must be performed. Nowadays there is no summary available on the injection mechanisms of the biofuels, the behavior of fuel drops in fuel sprays and the distinctive features of the behavior of biofuels compared to regular fuels. As the drop size is an important factor in determining fuel evaporation and combustion in engine cylinder, then this analysis may provide some explanations about the formation of fuel sprays of biofuels and about the characteristics of the combustion of biofuels.

Therefore, the aim of the article is to provide an overview of the behavior of fuel drops and their size in fuel sprays when various biodiesels (hereinafter biofuels) are used. The reason for determining of drop size and behavior is the possible assessment of the quality of air-fuel mixture in order to explain the reduction of soot emission when biofuels are used. The theoretical part is based on the fuel drops' formation models, which are used to perform the calculations to describe the behavior of various biofuels in the fuel spray. The article describes the formation of fuel drops, points out their impact parameters and analyses the behavior of the drops of biofuels in the fuel spray.

The main theoretical assumptions on which this paper is based:

1. Sprayed fuel drops are being considered as (symmetrical) physical bodies, which have the ability to bounce, coalesce and separate from each other [61, 62, 63, 64, 65].
2. The ability to bounce, coalesce and separate from each other is dependent of the intrinsic and the environmental physical properties (pressure, temperature, etc.) [66, 67, 68].
3. The spraying process is considered as a two-phase event: primary breakout of the fluid and the formation of droplets. Several theories describe this event: WAVE-RT, WAVE-TAB, WAVE-KH, etc., each with a respective mathematical interpretation [69, 70, 71].

The detailed mathematical background will be discussed in Sections 3 (Parameters describing fuel drop formation and collision), 4 (Fuel drop size after leaving the injector), 5 (Hybrid

breakout model) and 6 (Mathematical representation of reflexive and stretching separation).

The topic of the article is related to the scope of the Journal of the Power and Technologies by the theme of renewable energy. The article provides an overview of the behaviour of biofuels' drops in the spray, what is more, it supplements the database of the journal with explanations of the problems of biofuels' spray.

1. Problem description

When biofuels, for example, FAME, is used as fuel in a diesel engine, then generally the soot level decreases in the exhaust gas and the number of soot particles, emission of carbon dioxide and nitrogen compounds increases in the exhaust gas. The increased level of nitrogen compounds and CO2 and the reduction of soot level is caused by the more efficient combustion of biofuels (HVO, FAME) in the engine. The more efficient combustion is justified by the biofuel's oxygen content, which improves the combustion of the fuel. In addition, sources discuss thoroughly the carbon-hydrogen ratio in the fuel [20, 31, 32, 39, 58, 59, 60].

Unfortunately, the reasons given in these scientific sources are not in conformity with generally known theories, because, for example, the diesel engine always works with lean mixture, where the value of the air-fuel equivalent ratio is usually greater than 1.25. For turbo engines, this value is greater than ˜4 [72]. Therefore, the cylinder of a diesel engine contains theoretically sufficient amount of oxygen for the complete combustion of fuel. In addition, the engine tests of HVO fuel are in contradiction with the FAME results. The HVO fuel does not contain oxygen, but the soot level in the emission gas is reduced. It is also questionable how the carbon-hydrogen ratio affects the emission gas. If we presume that for the engine to work on same load, the same amount of energy must be added and this is derived from the fuel carbon-hydrogen ratio, then the fuel added to the engine has always the same magnitude of carbon-hydrogen atoms. Further, the test results show a contradiction in fuel properties and fuel behavior during injection.

Table 1 compares the physical properties of diesel fuel (DF), HVO and FAME obtained by testing according to the standard EN-590. The properties of gasoline are obtained from source [73]. In order to avoid the fuel's possible different properties listed in sources, the data listed in the table has been obtained by testing. In the table, gasoline has been given as reference fuel for comparing low viscosity fuels with high viscosity fuel. Table 1 shows, for example, that the viscosity of HVO and FAME is greater than that of diesel fuel. According to general knowledge, when the viscosity of the fuel increases, the fuel drop size in the fuel spray should increase, which also increases the combustion time. The longer combustion time prevents large fuel drops from combusting completely, which increases the level of soot in the emission gas. In our case, this is in contradiction with the results given in previous studies. When comparing fuel weight fractions, then HVO fuel contains lighter fractions compared to diesel fuel. It can be said about the FAME fuel that this fuel contains significantly more heavy fractions compared to diesel fuel (when the temperatures of the evaporated parts (10%-90%) of fuel are compared). Likewise, the heavy fractions of fuel need more time for combustion. Therefore, the soot level of emission gas of the FAME fuel must be at least in the same magnitude as diesel fuel. The following chapters provide an overview the behavior of fuel drops in the fuel spray and describe the effect of the properties of biofuels on the fuel drop size.

Table 1. Properties of diesel fuel and biofuels used in diesel engines.

Parameter	Unit	Method	GAS
Density (15 °C)	kg/m3	EN ISO 12185	703
Fractional distillation			
Initial boiling point (IBP)	°C		
BP 10%	°C		
BP 20%	°C		
BP 30%	°C		
BP 50%	°C		
BP 60%	°C		
BP 70%	°C		
BP 80%	°C		
BP 90%	°C		
BP 95%	°C		
Evaporated at temperature (180 °C)	vol%		
Evaporated at temperature (250 °C)	vol%		
Evaporated at temperature (350 °C)	vol%		
Final boiling point (FBP)	oC		
Recovery	vol%		
Residue	vol %		
Loss	vol %		
Kinematic viscosity (40 °C)	mm2/s	EN ISO 3104	1.223
Dynamic viscosity (40 °C)	mPa·s	EN ISO 3104	0.86
Sulfur content	mg/kg	EN ISO 20846	
Kinematic viscosity (90 °C)	mm2/s		0.53
Dynamic viscosity (90 °C)	mPa·s		0.038
Surface tension (90 °C)	N/m		0.018
Density (90 °C)	kg/m3		709

Based on the problem, the method of literature overview and the modeling of the fuel drops behavior in the spray are chosen. Theoretical calculations give an opportunity to evaluate experimental results of the behavior of different biofuels in the fuel spray and explain the .reasons of the problem.

1. Parameters describing fuel drop formation and collision

When fuel is sprayed, the fuel spray is broken down into drops. As the fuel drops move in the fuel spray, the drops are broken down by air resistance and the collision of drops occurs, which changes the drop size *dc* (Sauter Mean Diameter, *SMD -d32*).

Three dimensionless parameters are used for the modelling of the decomposition of fuel drops:

Weber number *We*

$$We = \frac{\rho \bullet |v_1 + v_2|^2 \bullet (D_1 - D_2)}{\sigma} \quad (1)$$

where ϱ is the fluid's density (kg/m3),$v1$ and $v2$ are the respective speeds of smaller and bigger drops (m/s),$D1$ and $D2$ are the respective diameters of the drops (m) and σ is the fluid's surface tension factor (N/m).

Impact parameter B

$B = \frac{2b}{(D_1+D_2)}$ (2)

where b is the distance from the centre of one drop to the relative velocity vector placed to the centre of the other drop (m).B = 0 corresponds to the frontal impact of the drops and B= 1 corresponds to the situation in which the drops graze each other (Fig. 1).

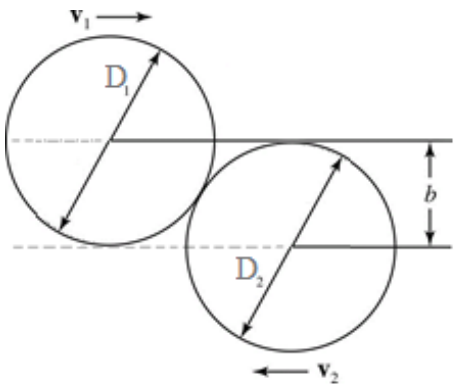

Figure 1: Couldn't find a caption, edit here to supply one.

Fig. 1. An explanation of the impact parameter B , where$b$ is the distance from the centre of one drop to the relative velocity vector placed to the centre of the other drop (m),$v1$ and $v2$ are the respective speeds of smaller and bigger drops (m/s) and$D1$ and $D2$ are the respective diameters of the drops (m).

Drop size ratio γ

$\gamma = \frac{D_2}{D_1}$ (3)

$\Delta = \frac{D_1}{D_2}$ (4)

Depending on these three parameters, the collision of two drops may have five possible results [61, 62, 63, 74, 75, 76, 77, 78, 79, 80]:

1. slow coalescence,
2. bounce,
3. coalescence,
4. reflexive separation,
5. stretching separation.

The possible results of the collision of drops have been given in Fig. 2 [81].

In case of reflexive and stretching separation, the satellite drops are formed in addition to daughter drops. The mechanism of the formation of satellite drops is described by the Plateau-Rayleigh instability [82, 83]. The diameter d sat and number$N$ sat of satellite drops can be modelled using the Munnannur-Reitz model [84], whereby both of these depend on the Weber number. Fig. 3 depicts the possibilities $B = f$ (We) as a diagram [66].

Situation B = 0 corresponds to the frontal impact of two drops. The colliding drop size ratio in this diagram is γ = 1, which corresponds to the situation in which the colliding drops have equal diameters. If γ is increased to values 100 and more, then cohesion forces increase the probability of coalescence of the drops. If the ambient pressure p is increased, then the slow coalescence area disappears as it becomes harder during collision to squeeze out the gas (air) between the drops.

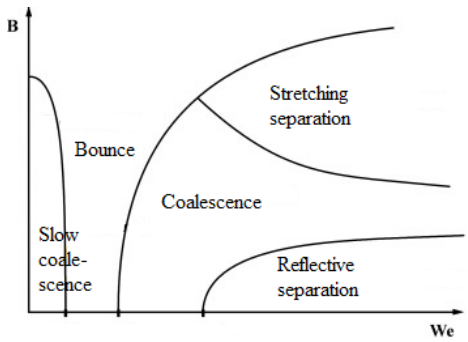

Figure 2: Couldn't find a caption, edit here to supply one.

Fig. 3. Possible results of the collision of two drops at ambient temperature T = 300 K and pressure p = 1 atm [66].

From the point of view of biofuels, it is important the size of the drop during spraying depends mostly on their physical and chemical properties, density, surface tension, viscosity. These properties of fuels are the main causes why the different fuels form different properties of air-fuel mixtures in engine cylinder and why the combustion properties are different. The fuel drop size is crucial during the combustion of air-fuel mixture by affecting directly the combustion efficiency and engine exhaust gas.

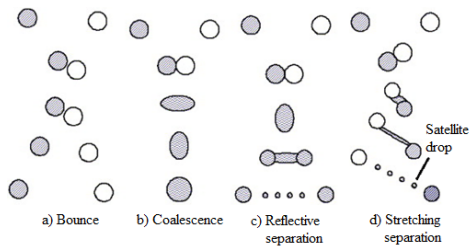

Figure 3: Couldn't find a caption, edit here to supply one.

Figure 2. Drop-drop collision mechanisms [81].

1. **Fuel drop size after leaving the injector**

The size of the fuel drop after leaving the injector can be expressed as follows [85]:

$d_c = \frac{2\pi B_d \sigma \lambda_m}{\rho_a U_T^2}$ (5)

where Bd is a parameter that depends on the injector nozzle's geometry. In previous works [86] the value ofBd was chosen Bd = 0.62,σ – fluid's (gasoline, DF, HVO, FAME) surface tension factor (N/m), λ m – fluid's Taylor viscosity parameter,ϱ a –

density of outer or gas environment (kg/m3), U T – velocity of the fastest unstable wave of the spray (m/s), wherebyUT is in linear correlation with the initial velocity of the injected spray. Here U T = 0,25 [?]U 0, where U 0 is the initial velocity of the spray (m/s).

It is possible to obtain the mean diameter of drops leaving the injector or Sauter mean diameter (*SMD*) by using equation 5 and data listed in sources [66, 87]. Table 2 presents some illustrative *SMD* values according to various authors.

Table 2. Values of *SMD* from chosen authors.

Author	Qian[66]	Qian[66]
Environment	Nitrogen	Nitrogen
Pressure p (atm)	1.0	2.4
Temperature T (K)	300	300
Environment (gas) density $\varrho\gamma$ (kg/m3)	-	-
Spray diameter $d0$ (μm)	246	246
Fuel	Tertadecane (DF)	Tertadecane (D
Fuel density $\varrho\lambda$ (kg/m3)	763	763
Surface tension factor σ (N/m)	2.18·10-2	2.18·10-2
SMD (μm)	9.5	4.1

Here it should be pointed out that in addition to *SMD* , other parameters are used to describe the drops, for example,$d10$, $d20$,$d30$, $d43$ (Herdan Mean Diameter or *HMD*), etc. [88, 89]. *SMD* is related to the volume-area ratio and describes the mean size of fuel drops in the fuel spray. Therefore, this parameter is used in most of the equations related to the formation of air-fuel mixture and combustion of fuel sprays and air-fuel mixtures.

Sources [90, 91, 92] point out several methods for determining the *SMD* of drops leaving the injector. The following equations are common for diesel engines:

$$SMD = 4,12 d \mathrm{Re}^{0,12} \mathrm{We}^{-0,54} \left(\frac{\mu_f}{\mu_g}\right)^{0,54} \quad (6)$$

$$SMD = 0,38 d \mathrm{Re}^{0,25} \mathrm{We}^{-0,32} \left(\frac{\mu_f}{\mu_g}\right)^{0,37} \left(\frac{\rho_f}{\rho_g}\right)^{-0,47} \quad (7)$$

$$SMD = 8,7 \left(\mathrm{Re}_l \mathrm{We}_l\right)^{-0,28} d_0 \quad (8)$$

where Re and We are respective Reynolds and Weber numbers,μ – fuel dynamic viscosity (Pa·s), ϱ – density (kg/m3),$d0$ is the diameter of injector's opening (m). Index "f " denotes "fluid" and "g " denotes "gas".

In addition to the abovementioned sources there are other authors [81, 93, 94, 95, 96], who give a theoretical and experimental assessment of *SMD* in their work. Results are mostly given as functions of time and distanceSMD = f(t) and SMD = f(x) as the sprayed fuel drops constantly change their size (coalescence, reflexive separation and stretching separation with satellite drops). The*SMD* values of these works remain in the range of 40–100 μm.

1. Hybrid breakout model (WAVE)

The size of fuel drops changes continuously after leaving the injector depending on ambient temperature, drop's velocity, distance etc. The size and their change can be described using the WAVE (hybrid breakout) models. The WAVE models can be used to describe breakout of various biofuels (HVO, FAME) and the size of their drops in the fuel spray.

The breakout of fuel spray that has left the injector takes place in two stages. First, the fuel is sprayed into drops (primary breakout). Then, the drops break out once again due to aerodynamic forces (secondary breakout) [97, 98, 99, 100, 101]. This dual-stage process can be described according to hybrid breakout model of drops (Fig. 4).

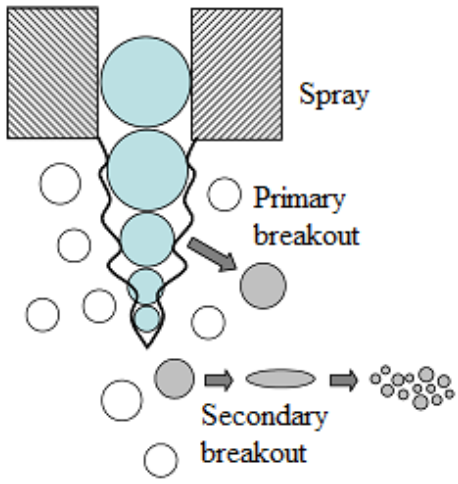

Figure 4: Couldn't find a caption, edit here to supply one.

Fig. 4. Schematic drawing of hybrid breakout model [81].

There are several hybrid breakout models: WAVE-RT [69, 70, 102, 103, 104, 105], WAVE-TAB [71, 106, 107, 108], WAVE-DDB [109, 110], WAVE-ACT [111], etc. Various models have been compared in the overview article [112]. The relations used in this study are given according to the WAVE-RT model which was used most widely in research. According to the original WAVE model, the surface of the fluid leaving the injector develops Kelvin-Helmholtz instability, which lead to the emerging of sinusoidal surface waves. These waves lead to the separation of the unstable part of fluid from the spray, which leads to the generation of drops. According to the WAVE model [71, 109], the drop growth speedKH and corresponding wavelengthΛKH is represented as follows:

$$\frac{\Lambda_{\mathrm{KH}}}{r} = 9,02 \frac{\left(1+0,45Z^{0,5}\right)\left(1+0,4T^{0,7}\right)}{\left(1+0.87\mathrm{We}_g^{1,67}\right)^{0,6}} \quad (9)$$

$$\Omega_{\mathrm{KH}} \left(\frac{\rho_f r^3}{\sigma_f}\right)^{0.5} = \frac{\left(0,34+0,38\mathrm{We}_g^{1,5}\right)}{(1+Z)\left(1+1,4T^{0,6}\right)} \quad (10)$$

The relations 9 and 10 contain members which are expressed as follows:

$$d_c = 2B_0 \Lambda_{\mathrm{KH}} \quad (11)$$

$$\tau_{\mathrm{KH}} = \frac{3,726 B_1 r}{\Omega_{\mathrm{KH}} \Lambda_{\mathrm{KH}}} \quad (12)$$

where We and Re are the Weber number and Reynolds number. While the Weber number determines the nature of drops after the possible coalescence of drops, then the Reynolds number characterizes the distribution of drops in a gas environment.

$$Z = \frac{\sqrt{\mathrm{We}_f}}{\mathrm{Re}_f} \quad (13)$$

$$T = Z\sqrt{\mathrm{We}_g} \quad (14)$$

$$\mathrm{Re}_f = \frac{\rho_f \mathrm{vr}}{\mu_f} \quad (15)$$

were $\varrho\varphi$ and $\varrho\gamma$ are the densities of fluid and gas (kg/m3); v – fluid velocity (m/s). In this context, the value of v can be considered equal to velocity of the spray leaving the injector, r – radius of fluid spray leaving the injector (m), $\mu\varphi$ – dynamic viscosity of fluid (Pa·s), $\sigma\varphi$ and $\sigma\gamma$ – surface tension of fluid and gas (N/m).

The physical and chemical properties of fuel affect the fuel drop size in the fuel spray. Thus, their influence has been described in detail in the following Fig. 5–8. In this research, the range of variated parameters are chosen accordingly to describe the diesel engine work mode. Values of the fuels parameters, by example dynamic viscosity µf, density etc. are used on condition of the engine.

The following relations are for finding the diameter dc of the drop leaving the injector's spray and drop breakout time τKH [71, 109]:

$$\mathrm{We}_f = \frac{\rho_f v^2 r}{\sigma_f} \quad (16)$$

$$\mathrm{We}_g = \frac{\rho_g v^2 r}{\sigma_f} \quad (17)$$

where $B0$ and $B1$ are empirical constants with values $B0$ = 4.5 and $B1$ = 40. Various sources [71, 113, 114] give different values to the constants $B0$ and $B1$. The values of $B1$ are usually within the range 1-60 depending on the characteristics of the injector.

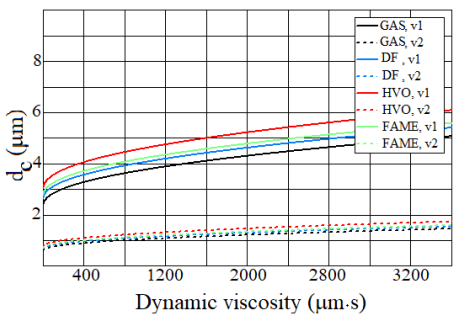

Figure 5: Couldn't find a caption, edit here to supply one.

Fig. 5. Dependency between the diameter dc of the drop leaving the injector and fluid's dynamic viscosity µf at two different velocities v of the spray ($v1$ = 200 m/s, $v2$ = 400 m/s), for four different fuel types. The x -axis value range 0-3600 µPa·s corresponds to typical viscosities of fuels at temperatures 40 °C and 90 °C (Table 1).

Equation 11 contains the member ΛKH , which contains the fluid's dynamic viscosity $\mu\varphi$. Therefore, it is possible to represent graphically the dependency dc of the drop leaving the injector and fluid's dynamic viscosity $\mu\varphi$ for various fuels (Fig. 5). The diagrams of Fig. 5 presume that the surface tension and density of fuel does not change. The density of the gas environment is 17 kg/m3, injector's opening's diameter 100 µm. According to sources [115, 116, 117, 118, 119, 120, 121], the physical parameters of the fuels correspond to the temperature 90 °C.

Fig. 5 shows that as the dynamic viscosity increases, the drop size in the air-fuel mixture also increases. An important factor having an effect on the drop size is the velocity of the fuel spray. The higher the velocity of the fuel spray, the smaller the diameter of the drop. Dynamic viscosity has a bigger effect on the change of fuel drop size in case of lower velocity fuel spray. For example, in case of the velocity of 400 m/s of the drop of any fuel, the change of fuel drop size is relatively smaller than compared to the speed of 200 m/s. Likewise, the physical and chemical properties of fuels have an effect on the drop size mostly at the lower velocity of the spray $v1$= 200 m/s. When we compare the fuel spray of gasoline and HVO fuel at spray velocity of 200 m/s, then, for example, we can see that at the dynamic viscosity's value of 1600 µPa the difference of drop size is ˜1 µm (25%). At drop velocity of $v2$ = 400 m/s the change of drop size is 0.2 µm (16%).

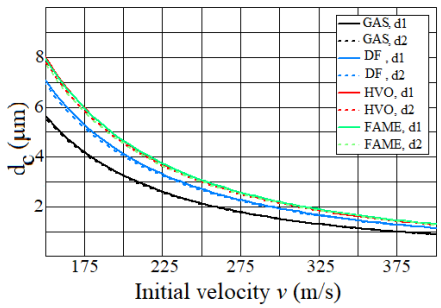

Figure 6: Couldn't find a caption, edit here to supply one.

Fig. 6. The dependency between the diameter dc of the drop leaving the injector and fluid's initial velocity v in case of two different diameters d of injector's opening ($d1$ = 100 µm, $d2$ = 300 µm) in case of four different fuel types. The x -axis value range 150-400 m/s corresponds to typical velocities of fuel drops in engine practice.

The dependency between the diameter dc of the drop leaving the injector and fluid's initial velocity v has been given in Fig. 6 and the diameter dc of the drop leaving the injector and injector's diameter d has been given in Fig. 7. Here the density of the gas environment was 17 kg/m3 and the physical parameters of the fuels correspond to the temperature 90 °C.

Fig. 6 shows that as the drop's velocity increases, the drop's size decreases. Here it is important to point out that the diameter of the injector's opening does not have a significant effect on the drop's size. As the drop's velocity is doubled, its size decreases ˜3 times. The physical and chemical properties have an effect on the fuel drop's size. For example, as the fuel's kinematic viscosity increases, the drop size increases (starting from gasoline to FAME or HVO fuel). It is important that in case FAME and HVO fuels no drop size difference is evident. This is can be caused by the difference between dynamic viscosities and surface tensions. The dynamic viscosity of the FAME fuel is greater than that of the HVO fuel, however, the surface tension of the HVO fuel is greater than that of the FAME fuel. Therefore, the change of the drop size is within the same magnitude. Fig. 7 shows that the diameter of the injector's opening does not have a significant effect on the drop size in spray re-

gardless of the spray velocity.

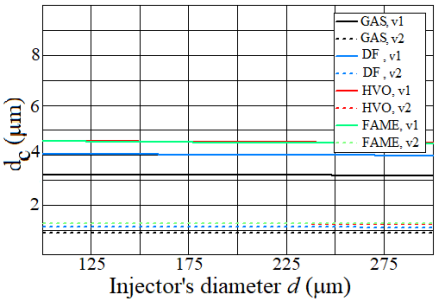

Figure 7: Couldn't find a caption, edit here to supply one.

Fig. 7. Dependency between diameter $dc$of the drop leaving the injector and injector's diameter d at two spray velocities v ($v1$ = 200 m/s,$v2$ = 400 m/s) in case of four different fuel types. The x -axis value range 100-300 μm corresponds to typical fuel injector diameters.

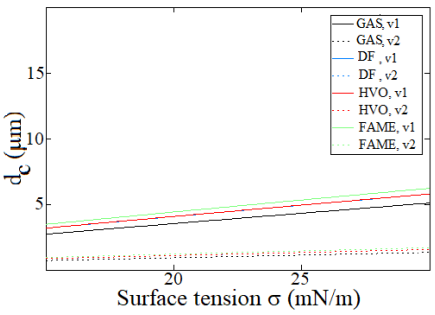

Figure 8: Couldn't find a caption, edit here to supply one.

Fig. 8. Dependency between diameter $dc$of the drop leaving the injector and fluid's surface tension σ at two spray velocities v ($v1$ = 200 m/s,$v2$ = 400 m/s). The x -axis value range 15-30 mN/m corresponds to typical surface tensions of fuels at temperatures 90 °C (Table 1).

Fig. 8 shows the fuel drop size according to the surface tensions of fuels at various spray velocities. The figure shows that as the surface tension increases, the drop size also increases. It is important that the fuel's surface tension has a greater effect on drop size at lower velocities ($v1$ = 200 m/s) than at higher velocities ($v2$ = 400 m/s).

In conclusion, it can be claimed that the fuel drop's size is significantly influenced by the velocity v of the fuel spray, dynamic viscosity μ , density ϱ and surface tension factorσ . In order to characterize the drops formed during the preparation of the air-fuel mixture, these parameters must be viewed separately and the physical and chemical properties of each fuel shall be taken into account and projected into the working conditions of a real engine.

The data in Table 3 takes into account that the temperature of the sprayed fuel and the density of the spraying environment are comparable to the actual environment in the engine cylinder. Here the temperature of the sprayed fuel was chosen to be 90 °C [122], which corresponds to the temperature of the working engine. The density of the spraying environment was 17 kg/m3.

1. **Mathematical representation of reflexive and stretching separation**

The description of the collision of fuel drops is based on the assumption that the drops move confluently and collisions only take place when one fuel drop catches up with another one in the fuel spray. The movement, collision and separation of drops is described in Fig. 9 [123]. The calculations are based on the assumption that after the collision of drops in the fuel spray, the reflexive and stretching separation occur.

Reflexive separation occurs in case of large Weber numbers We and low values of the impact parameter B . This means either frontal impact or a similar situation. If the Weber number is large (>100) and the impact parameter is growing, then stretching separation shall become dominant after the collision of the drops. The impact parameter B also determines the number of collisions [124].

In order to describe these two processes, the kinetic energy of two colliding drops and the law of the conservation of the surface energy of the temporarily joined drops shall be used. The Weber number for separation of drops for the two processes can be described as follows [123]:

$$textWe_{\text{reflection}} > \frac{3\left[7\left(1+\Delta^3\right)^{\frac{1}{3}} - 4\left(1+\Delta^2\right)\right]\Delta\left(1+\Delta^3\right)^2}{\Delta^6\eta_1 + \eta_2}$$

(18)

which applies to reflexive separation; and

$$textWe_{\text{stretching}} > \frac{4\left(1+\Delta^3\right)^2\left[3\left(1+\Delta\right)\left(1-B\right)\left(\Delta^3\varphi_1+\varphi_2\right)\right]^{\frac{1}{2}}}{\Delta^2\left[\left(1+\Delta^3\right)-\left(1-B^2\right)\left(\varphi_1+\Delta^3\varphi_2\right)\right]}$$

(19)

which applies to stretching separation. The dimensionless constants$?1$, $?2$ and ξ (Table 3) are used for simplifying the calculations and these are obtained as follows:

$$\eta_1 = 2\left(1-\xi\right)^2\left(1-\xi^2\right)^{\frac{1}{2}} - 1 (20)$$

$$\eta_2 = 2\left(\Delta-\xi\right)^2\left(\Delta-\xi^2\right)^{\frac{1}{2}} - \Delta^3 (21)$$

$$\xi = \frac{1}{2}B\left(1+\Delta\right) (22)$$

The dimensionless values of $\varphi 1$ and$\varphi 2$ are used for describing the stretching separation and these values denote the respective proportions of spatial areas in joined drops. The values of $\varphi 1$ and$\varphi 2$, parts of interaction volumes$V1i$, $V2i$ and interaction volume Vi can be represented as follows:

$$\varphi_1 = \{ \begin{array}{l} 1 - \frac{1}{4^3}\left(2\Delta-\lambda\right)^2\left(\Delta+\lambda\right) \\ \frac{\lambda^2}{4^3}\left(3\Delta-\lambda\right) \end{array} (23)$$

$$\varphi_2 = \{ \begin{array}{l} 1 - \frac{1}{4}\left(2-\lambda\right)^2\left(1+\lambda\right) \\ \frac{\lambda^2}{4}\left(3-\lambda\right) \end{array} (24)$$

KEseparation describes the separation kinetic energy and *PEcoalescence* the surface tension energy which is needed to sustain the coalescence of the two drops. In case of reflexive separation, the *KEseparation*and *PEcoalescence* can be presented as follows:

$$textKE_{\text{separation}} = \sigma\pi D_2^2 \left[\left(1+\Delta^2\right) - \left(1+\Delta^3\right)^{\frac{2}{3}} + \frac{\text{We}}{12\Delta\left(1+\Delta^3\right)^2} \left(\Delta^6\eta_1 + \eta_2\right) \right]$$

(30)

$$\text{PE}_{\text{coalescence}} = 0.75\sigma\pi \left(D_1^3 + D_2^3\right)^{\frac{2}{3}} (31)$$

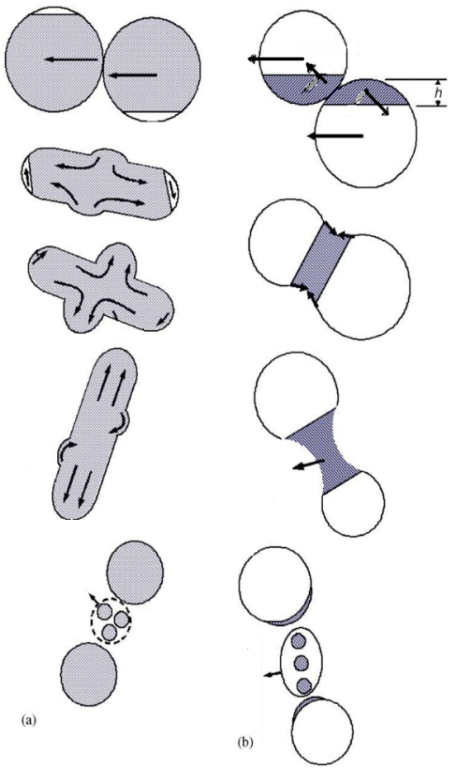

Figure 9: Couldn't find a caption, edit here to supply one.

Fig. 9. Schematic representation of (*a*) reflexive and (*b*) stretching separation [123].

Table 3. The calculated values of the Weber numbers *We*(equations 18 and 19) in case of the different diameters*d1* , *d2* of the colliding drops and impact parameter *B* .

	1	2	3	4	5	6
Διαμετερ *δ1* (μμ)	**5**	**5**	**5**	**5**	**5**	**5**
Διαμετερ *δ2* (μμ)	**5**	**5**	**5**	**10**	**10**	**10**
Drop size ratio *γ*	1.0	1.0	1.0	2.0	2.0	2.0
Drop size ratio *Δ*	1.0	1.0	1.0	0.5	0.5	0.5
Distance *b* (μm) (Fig. 1)	0	100	400	0	150	600
Impact parameter *B*	**0**	**0.20**	**0.80**	**0**	**0.20**	**0.80**
?1	1	0.25	-0.95	1.00	0.43	-0.74
?2	1	0.25	-0.95	0.13	0	-
ξ	0	0.20	0.80	0	0.15	0.60

$V_{\mathrm{ji}} = \varphi_j V_j$ (25)

$V_i = V_{1i} + V_{2i}$ (26)

The dimensionless value of λ is expressed as follows:

$\lambda = (1 - B)(1 + \Delta)$ (27)

The selection criterion for the value of $\varphi 1$ is$h > r_1$ and $h < r_1$ respectively and the selection criterion for the value of $\varphi 2$ is $h > r_2$ and$h < r_2$ respectively. The value h marks the interaction height and is expressed as follows:

$h = \frac{1}{2}(D_1 + D_2)(1 - B)$ (28)

The values of $r1$ and $r2$express the radii of drops. In order to understand better the equations 18-27, several numeric examples have been given in Table 3.

Situation 1 describes the frontal impact ($B = 0$) of two drops with equal diameters. The Weber number values calculated according to equations 18 and 19 show that if *Wereflection*> 4.9, then reflexing separation takes place with no stretching separation occurring. If none of the separations occur according to the calculations of Table 3, then it must be either the bouncing or coalescence of the drops. This model does not discuss these cases further.

If the value of the impact parameter B is greater ($B = 0.20$), then it corresponds to a situation in which two drops collide under conditions similar to a frontal impact. In such cases the reflexive separation starts to occur from the value*Wereflection* > 19.3 onwards and stretching separation *Westretching* > 167.8.

In situation 3 the drops nearly graze each other ($B = 0.80$). Reflexive separation does not occur in this situation. Stretching separation will occur already with smaller Weber numbers (*Westretching* > 4.2).

Situation 4 constitutes a frontal impact of two drops ($B = 0$), whereby one of the drops has twice the diameter of the other one (size ratio of colliding drops is $\gamma = 0.5$). Reflexive separation will occur staring from the value *Wereflection*> 30.8 and stretching separation*Westretching* > 38.7. In comparison to situation 1, the greater values of the Weber numbers are caused by the fact that the larger drop swallows the smaller one. In case of lower*We* values; surface tension causes the domination of coalescence.

In situations 5 and 6 the size ratio of colliding drops is stillγ = 0.5, but the impact parameter has been increased to B= 0.20 and B = 0.80 respectively. Reflexive separation does not occur in any of the situations. In situation 5, the stretching separation will start occurring from *Westretching*> 153.4 onwards and in situation 6*Westretching* > 5.4.

It should be noted that in case of stretching separation, the interaction height h and interaction volumeVi are much smaller than in case of reflexive separation. In case of reflexive separation, the total volume of joined drops is equal to the interaction volume.

The separation volume coefficient Cv is introduced to determine the volume of the fluid separating from two colliding drops and it is defined as the ratio of the volume separating from the two drops and the interaction volume. It is presumed [125] thatCv is equal to the energy needed for the separation and the total energy of the two colliding drops:

$C_v = \frac{\mathrm{KE_{separation}} - \mathrm{PE_{coalescence}}}{\mathrm{KE_{separation}} + \mathrm{PE_{coalescence}}}$ (29)

	1	2	3	4	5	6
λ	2	1.60	0.40	1.50	1.20	0.30
$\varphi 1$	1	0.90	0.10	0	0.86	0.22
$\varphi 2$	1	0.90	0.10	0.84	0.65	0.06
Wereflection (eq. 18)	**4.9**	**19.3**	**-**	**30.8**	**-**	**-**
Westretching (eq. 19)	**-**	**167.8**	**4.2**	**38.7**	**153.4**	**5.4**

In case of stretching separation the *KEseparation*and *PEcoalescence* can be presented as follows:

$$textKE_{\mathrm{separation}} = \frac{1}{2}\rho\,(v_1 + v_2)^2\,V_2 \left\{ \frac{\Delta^3}{(1+\Delta^3)^2} \left[\left(1+\Delta^3\right) - \left(1 - B^2\right)\left(\varphi_1 + \right.\right.\right.$$

(32)

$\mathrm{PE_{coalescence}} = \sigma \left[2\pi V_2 D_2 \lambda \left(\Delta^3 \varphi_1 + \varphi_2 \right) \right]^{\frac{1}{2}}$ (33)

$V2$ in equations 32 and 33 marks the volume of the second drop before the collision.

Taking into account the separation volume coefficient in equation (29) and the values of $\varphi 1$ in equation (23) and$\varphi 2$ in equation (24), the diametersdc of the drops after the collision can be calculated as follows:

$d_{c1} = (1 - C_v \varphi_1)^{\frac{1}{3}}\, d_1$ (34)

$d_{c2} = (1 - C_v \varphi_2)^{\frac{1}{3}}\, d_2$ (35)

where $d1$ and $d2$ are the respective diameters of the first and second drop before the collision,$dc1$ and $dc2$ are the respective diameters of the first and second drop after the collision.

Fig. 10 shows the relative diameters of drops for different impact parameters. This illustrates the change of the size of the drops breaking out and colliding. Calculations have been performed for four fuel types. In case of the relation $\Delta 1 = 0.5$, the ratio of the sizes of the formed drop and the collided drop changes. This means that in case of a small impact parameter, the size of the drop formed after the collision is a smaller percentage of the drop size before collision in comparison to the values of greater impact parameters. In simpler terms this means that the small values of the impact parameter result in smaller drops after the collision than compared to greater values of the impact parameter. It is important about the relation of $dc\ /d$ for various fuels that the ratio of change of the drop size does not change significantly for the value $\Delta 1$. Here we can conclude that the injection of fuels with different physical and chemical properties into the engine cylinder does not result in a significant difference of the quality of the air-fuel mixture.

In a situation where $\Delta 2 = 1$, the influence of the impact parameter on the relative drop diameter in the fuel spray changes significantly. It can be seen from the figure that at the impact parameter's values B = 0–0.15 the drop size ratio increases as the impact parameter increases. At the values B = 0.15-1 the relative diameter of the drops increases as the value of the impact parameter increases. It can be further seen from the graph that at the impact diameter value of B = 0.22, the fuel properties have an influence on the drop size. For example, at the value of $B = 0.15$ the drop of gasoline after breakout is ˜2.5% smaller than compared to the HVO fuel. The comparison of FAME fuel and diesel fuel does not reveal a significant change

in drop size ratio. The drop size ratio of diesel fuel remains on the same level as gasoline and FAME fuel.

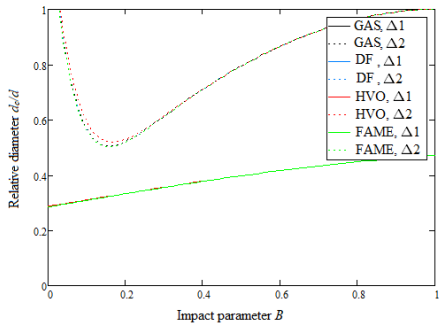

Figure 10: Couldn't find a caption, edit here to supply one.

Fig. 10. The dependency of the relative diameterdc/d of a drop that formed after the collision and the impact parameter B at two different colliding drop diameter ratios Δ (equation 4) ($\Delta 1$ = 0.5,$\Delta 2$ = 1.0) in case of four different fuel types.

Fig. 10 was obtained with the parameters $v1$ =$v2$ = 200 m/s and the physical parameters of the fuels correspond to the temperature of 90 °C. Fig. 10 shows that the drop size can differ in the air-fuel mixture at various values ofΔ . It can be concluded that the air-fuel mixture of fuels with high viscosity (for example, HVO) contains somewhat larger drops than the mixture of low viscosity fuel. At the same time, the drops of FAME fuel are in the same magnitude as gasoline and diesel fuel. In addition to viscosity, another important influencing factor is surface tension. At low values of B , the ratio dc/d is mostly determined by the fuel's surface tension forces. If the value of$B$ is greater, then the interaction volume remains smaller, which means that the ratio dc/d is also greater.

Table 4 was prepared to illustrate better the breakout of fuel drops. The table gives the drop sizes of various fuels at various values of the impact parameter B . Table 4 exemplifies also a situation in which the colliding drops are equal. The physical parameters of fuels in Table 4 correspond to the temperature of 90 °C. In the first case (1), the value of Cv is negative for stretching separation, which means that the stretching separation does not occur. The positive value of Cv shows that reflexive separation takes place.

In the other cases (2-4) the reflexive and stretching separation of drops occurs. The main difference between the different cases is that when the impact parameter's value is B = 0.1, then the drop size of diesel fuel and gasoline is ~5 % smaller than that of HVO and FAME fuels. It can be deduced from here that the drop size in the air-fuel mixture of HVO and FAME fuels is somewhat greater than that of diesel fuel. Here the air-fuel mixture corresponds to the general knowledge, according to which the drop size in air-fuel mixtures of high viscosity fuels is greater. At the same time, it is not sure why the soot level of emission gas of biofuels is lower. If we presume that the use of FAME fuels results in lower soot levels in the exhaust gas mostly due to the oxygen content in the fuel, then what is the reason for the lower soot level of HVO fuel? In conclusion, it can be claimed that the drop size of biofuels in air-fuel mixture is somewhat larger. The approach of this article does not give the answer why the soot level in the engine's emission gas decreases when HVO and FAME fuels are used. At the same time, the results illustrate that there are no important differences in the quality of air-fuel mixture. In order to account for the reduced soot level, it is necessary to study experimentally the breakout of drops in the fuel spray, the effect of oxygen content on the combustion of fuel and the effect of various fuel fractions to the combustion process.

Table 4. Drop's diameter dc after collision and the value of separation coefficientCv in case of a collision of two drops with equal diameters.

Diameter $d1$ (μm)	5.0
Diameter $d2$ (μm)	5.0
Velocity $v1$ (m/s)	100
Velocity $v2$ (m/s)	100
Impact parameter B	**0**
Interaction volume to volume ratio Vi/V	1.00
Gasoline (GAS)	**Gasoline (GAS)**
Weber number We	7878
Separation volume coefficient Cv (eq 29) (*reflexing*)	0.99
Separation volume coefficient Cv (eq 29) (*stretching*)	-1.00
Drop size dc after separation (μm)	5.0
Diesel Fuel (DF)	**Diesel Fuel (DF**
Weber number We	9111
Separation volume coefficient Cv (eq 29) (*reflexing*)	0.99
Separation volume coefficient Cv (eq 29) (*stretching*)	-1.00
Drop size dc after separation (μm)	5.0
HVO	**HVO**
Weber number We	4762
Separation volume coefficient Cv (eq 29) (*reflexing*)	0.99
Separation volume coefficient Cv (eq 29) (*stretching*)	-1.00
Drop size dc after separation (μm)	5.0
FAME	**FAME**
Weber number We	5780
Separation volume coefficient Cv (eq 29) (*reflexing*)	0.99
Separation volume coefficient Cv (eq 29) (*stretching*)	-1.00
Drop size dc after separation (μm)	5.0

1. Summary

of the physical parameters of four different types of fuels (gasoline, diesel fuel, HVO, FAME) and phenomena related to these parameters, which include the spraying of fuel drops and the coalescence and collision of these drops. The fuel drop sizes after leaving the injector and after mutual collisions were calculated.

The results can be summarized as follows:

1. In the hybrid breakout model, spray velocity has a significant effect on the drop size. As the spray velocity increases, the size of drops decreases in the fuel spray. When considering the conditions under which fuel is sprayed in a working engine, then viscosity and surface tension are the factors that have a significant effect mostly at the low

spraying velocities. The higher the velocity of fuel spray, the lower the effect of viscosity and surface tension have on the drop size in the fuel spray. According to the used model, the diameter of the injection opening does not have an effect on the drop size in the fuel spray.

2. When biodiesel fuel is used, then according to the hybrid breakout model the drop size in the fuel spray is somewhat greater (˜12%). As the fuel spray velocity increases, the size ratio of drop increases.
3. When the drops collide in the fuel spray, then generally the drop size increases as the value of impact parameter B increases, if the drop size ratio of colliding drops is $\Delta = 0.5$. If the drop size ratio of colliding drops is $\Delta = 1$, then at the impact parameter's value of $B = 0.1$, the size of drops after breakout is the smallest. As the impact parameter B increases or decreases, the drop size in the fuel spray starts to increase. The physical and chemical properties of fuels do not have a significant effect on the drop size. Minor differences occur when drops of the same size collide at the impact parameter value range of $B = 0.5$–1.5.
4. The biodiesel air-fuel mixture contains somewhat larger drops than the air-fuel mixture of diesel fuel. The results show that the model used in study cannot be used to account for the reduction of the soot level of biodiesel fuel. This is due to the fact that the quality of the biodiesel air-fuel mixture is not significantly different from diesel fuel.

There are several further questions that need to be addressed:

1. How does the oxygen contained in the fuel influence the soot level of the combustion of the fuel?
2. How do the fuel drop sizes change in the injection chamber for the four types of fuel (gasoline, diesel fuel, HVO, FAME) both temporally and spatially?

The topic of the article is related to the scope of the Journal of the Power and Technologies by the theme of renewable energy. The article provides an overview of the behavior of biofuels' drops in the spray, what is more, it supplements the database of the journal with explanations of the problems of biofuels' spray.

1. References

[1] A. Kuut, R. Ilves, K. Kuut, V. Raide, K. Ritslaid, J. Olt, Influence of European Union Directives on the Use of Liquid Biofuel in the Transport Sector, Procedia Engineering (2017) 30–39.

[2] J. Xue, T. E. Grift, A. C. Hansen, Effect of biodiesel on engine performances and emissions, Renewable and Sustainable Energy Reviews 15 (2011) 1098–1116.

[3] H. Hazar, Effects of biodiesel on a low heat loss diesel engine, Renewable Energy 34 (2009) 1533–1537.

[4] A. N. Ozsezen, M. Canakci, A. Turkcan, C. Sayin, Performance and combustion characteristics of a DI diesel engine fueled with waste palm oil and canola oil methyl esters, Fuel 88 (2009) 629–636.

[5] Z. Utlu, M. S. Koçak, The effect of biodiesel fuel obtained from waste frying oil on direct injection diesel engine performance and exhaust emissions, Renewable Energy 33 (2008) 1936–1941.

[6] H. Ozgunay, S. Çolak, G. Zengin, O. Sari, H. Sarikahya, L. Yuceer, Performance and emission study of biodiesel from leather industry pre-fleshings, Waste Management 27 (2007) 1897–1901.

[7] C. Kaplan, R. Arslan, A. Surmen, Performance characteristics of sunflower methyl esters as biodiesel, Energy Sources Part A Recovery Utilization and Environmental Effects 28 (2006) 751–755.

[8] J. F. Reyes, M. A. Sepúlveda, PM-10 emissions and power of a diesel engine fueled with crude and refined biodiesel from salmon oil, Fuel 85 (2006) 1714–1719.

[9] H. Raheman, A. G. Phadatare, Diesel engine emissions and performance from blends of karanja methyl ester and diesel, Biomass and Bioenergy 27 (2004) 393–397.

[10] Y. Ulusoy, Y. Tekin, M. Cetinkaya, F. Karaosmanoglu, The engine tests of biodiesel from used frying oil, Energy Sources 26 (2004) 927–932.

[11] S.-H. Choi, Y. Oh, The emission effects by the use of biodiesel fuel, International Journal of Modern Physics B 20 (2006) 4481–4486.

[12] B.-F. Lin, J.-H. Huang, D.-Y. Huan, Experimental study of the effects of vegetable oil methyl ester on DI diesel engine performance characteristics and pollutant emissions, Fuel 88 (2009) 1779–1785.

[13] D. H. Qi, L. M. Geng, H. Chen, Y. Z. H. Bian, J. Liu, X. C. H. Ren, Combustion and performance evaluation of a diesel engine fueled with biodiesel produced from soybean crude oil, Renewable Energy 34 (2009) 2706–2713.

[14] M. Lapuerta, J. M. Herreros, L. L. Lyons, R. García-Contreras, Y. Briceño, Effect of the alcohol type used in the production of waste cooking oil biodiesel on diesel performance and emissions, Fuel 87 (2008) 3161–3169.

[15] H. Kim, B. Choi, The effect of biodiesel and bioethanol blended diesel fuel on nanoparticles and exhaust emissions from CRDI diesel engine, Renewable Energy 35 (2010) 157–163.

[16] X. Meng, G. Chen, Y. Wang, Biodiesel production from waste cooking oil via alkali catalyst and its engine test, Fuel Processing Technology 89 (2008) 851–857.

[17] A. Hull, I. Golubkov, B. Kronberg, J. van Stam, Alternative fuel for a standard diesel engine, International Journal of Engine Research 7 (2006) 51–63.

[18] M. Gumus, S. Kasifoglu, Performance and emission evaluation of a compression ignition engine using a biodiesel (apricot seed kernel oil methyl ester) and its blends with diesel fuel, Biomass and Bioenergy 34 (2010) 134–139.

[19] A. Pal, A. Verma, S. S. Kachhwaha, S. Maji, Biodiesel production through hydrodynamic cavitation and performance testing, Renewable Energy 35 (2010) 619–624.

[20] A. S. Ramadhas, C. Muraleedharan, S. Jayaraj, Performance and emission evaluation of a diesel engine fueled with methyl esters of rubber seed oil, Renewable Energy 30 (2005) 1789–1800.

[21] D. Sharma, S. L. Soni, J. Mathur, Emission reduction in a direct injection diesel engine fueled by neem-diesel blend, Energy Reports 31 (2009) 500–508.

[22] M. Guru, A. Koca, O. Can, C. Çınar, F. Şahin, Biodiesel production from waste chicken fat based sources and evaluation with Mg based additive in a diesel engine, Renewable Energy 35 (2010) 637–643.

[23] L. Zhu, W. Zhang, W. Liu, Z. Hunag, Experimental study on particulate and NOx emissions of a diesel engine fueled with ultra low sulfur diesel, RME-diesel blends and PME-diesel blends, Science of Total Environment 408 (2010) 1050–1058.

[24] K. Ryu, The characteristics of performance and exhaust emissions of a diesel engine using a biodiesel with antioxidants, Bioresource Technology 101 (2010) S78–S82.

[25] J. M. Luján, V. Bermúdez, B. Tormos, B. Pla, Comparative analysis of a DI diesel engine fuelled with biodiesel blends during the European MVEG-A cycle: Performance and emissions (II), Biomass and Bioenergy 33 (2009) 948–956.

[26] C. S. Cheung, L. Zhu, Z. Huang, Regulated and unregulated emissions from a diesel engine fueled with biodiesel and biodiesel blended with methanol, Atmospheric Environment 43 (2009) 4865–4872.

[27] S. J. Deshmukh, L. B. Bhuyar, Transesterified Hingan (Balanites) oil as a fuel for compression ignition engines, Biomass and Bioenergy 33 (2009) 108–112.

[28] A. Tsolakis, A. Megaritis, M. L. Wyszynski, K. Theinnoi, Engine performance and emissions of a diesel engine operating on diesel-RME (rapeseed methyl ester) blends with EGR (exhaust gas recirculation), Energy 32 (2007) 2072–2080.

[29] H. Raheman, S. V. Ghadge, Performance of compression ignition engine

with mahua (Madhuca indica) biodiesel, Fuel 86 (2007) 2568–2573.

[30] D. Agarwal, S. Sinha, A. K. Agarwal, Experimental investigation of control of NOx emissions in biodiesel-fueled compression ignition engine, Renewable Energy 31 (2006) 2356–2369.

[31] S. Puhan, N. Vedaraman, V. B. R. Boppana, J. Jeychandran, G. Sankarnarayanan, Mahua oil (Madhuca Indica seed oil) methyl ester as biodiesel-preparation and emissioon characterstics, Biomass and Bioenergy 28 (2005) 87–93.

[32] M. Canakci, Performance and emissions characteristics of biodiesel from soybean oil, Proceedings of the Institution of Mechanical Engineers, Part D: Journal of Automobile Engineering 219 (2005) 915–922.

[33] M. Canakci, J. H. van Gerpen, Comparison of engine performance and emissions for petroleum diesel fuel, yellow grease biodiesel, and soybean oil biodiesel, Transactions of the ASAE 46 (2003) 937–944.

[34] A. Senatore, M. Cardone, V. Rocco, M. V. Prati, A Comparative Analysis of Combustion Process in D.I. Diesel Engine Fueled with Biodiesel and Diesel Fuel, SAE paper 2000 1 (2000) 0691.

[35] M. J. Haas, K. M. Wagner, T. L. Alleman, R. L. McCormick, Engine performance of biodiesel fuel prepared from soybean soapstock: a high quality renewable fuel produced from a waste feedstock, Energy & Fuels 15 (2001) 1207–1212.

[36] P. K. Sahoo, L. M. Das, M. K. G. Babu, S. N. Naik, Biodiesel development from high acid value polanga seed oil and performance evaluation in a CI engine, Fuel 86 (2007) 448–454.

[37] B. Baiju, M. K. Naik, L. M. Das, A comparative evaluation of compression ignition engine characteristics using methyl and ethyl esters of Karanja oil, Renewable Energy 34 (2009) 1616–1621.

[38] F. Wu, J. Wang, W. Chen, S. Shuai, A study on emission performance of a diesel engine fueled with five typical methyl ester biodiesels, Atmospheric Environment 43 (2009) 1481–1485.

[39] Y. Ulusoy, R. Arslan, C. Kaplan, Emission characteristics of sunflower oil methyl ester, Energy Sources Part A 11 (2009) 906–910.

[40] C.-Y. Lin, R.-J. Li, Engine performance and emission characteristics of marine fish-oil biodiesel produced from the discarded parts of marine fish, Fuel Processing Technology 90 (2009) 883–888.

[41] D. Tziourtzioumis, L. Demetriades, O. Zogou, T. Stamatelos, Experimental investigation of the effect of a B70 biodiesel blend on a common-rail passenger car diesel engine, Proceedings of the Institution of Mechanical Engineers Part D Journal of Automobile Engineering 223 (2009) 685–701.

[42] M. Zheng, M. C. Mulenga, G. T. Reader, M. Wang, D. S.-K. Ting, J. Tjong, Biodiesel engine performance and emissions in low temperature combustion, Fuel 87 (2008) 714–722.

[43] M. E. Tat, J. H. van Gerpen, P. S. Wang, Fuel Property Effects on Injection Timing, Ignition Timing and Oxides of Nitrogen Emissions from Biodiesel-Fueled Engines, Transactions ASABE 50 (2007) 1123–1128.

[44] S. Kalligeros, F. Zannikos, S. Stournas, E. Lois, G. Anastopoulus, C. Teas, F. Sakellaropoulos, An investigation of using biodiesel/marine diesel blends on the performance of a stationary diesel engine, Biomass and Bioenergy 24 (2003) 141–149.

[45] M. Lapuerta, O. Armas, R. Ballestros, Diesel particulate emissions from biofuels derived from Spanish vegetable oils, SAE Paper 2002 1 (2002) 1657.

[46] H. Jung, D. B. Kittelson, M. R. Zachariah, Characteristics of SME biodiesel-fueled diesel particle emissions and the kinetics of oxidation, Environmental Science Technologies 40 (2006) 4949–4955.

[47] A. Monyem, J. H. van Gerpen, The effect of biodiesel oxidation on engine performance and emissions, Biomass and Bioenergy 20 (2001) 317–325.

[48] M. S. Graboski, R. L. McCormick, T. L. Alleman, A. M. Herring, The effect of biodiesel composition on engine emissions from a DDC series 60 diesel engine, National Renewable Energy Laboratory (2003) NREL/SR–510–31461.

[49] W. G. Wang, D. W. Lyons, N. N. Clark, M. Gautam, Emissions from nine heavy trucks fuelled by diesel and biodiesel blend without engine modification, Environmental Science and Technology 34.

[50] M. Cardone, M. V. Prati, V. Rocco, M. Seggiani, A. Senatore, S. Vitolo, Brassica carinata as an Alternative Oil Crop for the Production of Biodiesel in Italy: Engine Performance and Regulated and Unregulated Exhaust Emissions, Environmental Science & Technology 36 (2002) 4656–4662.

[51] N. Y. Kado, P. A. Kuzmicky, Progress in Energy and Combustion Science, National Renewable Energy Laboratory (2003) NREL/SR–510–31463.

[52] M. Lapuerta, O. Armas, R. Ballestros, M. Carmona, Fuel formulation effects on passenger car diesel engine particulate emissions and composition, SAE Paper 2000 (2000) 1850.

[53] O. Armas, J. J. Hernández, M. D. Cárdenas, Reduction of diesel smoke opacity from vegetable oil methyl esters during transient operation, Fuel 85 (2006) 2427–2438.

[54] K. Yamane, A. Ueta, Y. Shimamoto, Influence of physical and chemical properties of biodiesel fuels on injection, combustin and exhaust emission characteristics in a direct injection compression ignition engine, International Journal of Engine Research 2 (2001) 249–261.

[55] M. Lapuerta, O. Armas, J. M. Herreros, Emissions from a diesel-biodiesel blend in an automotive diesel engine, Fuel 1 (2008) 25–31.

[56] M. Lapuerta, O. Armas, R. Ballesteros, J. Fernández, Diesel emissions from biofuels derived from Spanish potential vegetable oils, Fuel 84 (2005) 773–780.

[57] K. Dincer, Lower Emissions from Biodiesel Combustion, Energy Sources 30 (2008) 963–968.

[58] G. Fontaras, G. Karavalakis, M. Kousoulidou, T. Tzamkiozis, L. Ntziachristos, E. Bakeas, S. Stournas, Z. Samaras, Effects of biodiesel on passenger car fuel consumption, regulated and non-regulated pollutant emissions over legislated and real-world driving cycles, Fuel 88 (1608-1617) 2009.

[59] T. Bohl, A. Smallbone, G. Tian, A. P. Roskilly, Particulate number and NOx trade-off comparisons between HVO and mineral diesel in HD applications, Fuel 215 (2018) 90–101.

[60] C. Vo, C. Charoenphonphanich, P. Karin, S. Susumu, K. Hidenori, Effects of variable O2 concentrations and injection pressures on the combustion and emissions characteristics of the petro-diesel and hydrotreated vegetable oil-based fuels under the simulated diesel engine condition, Journal of the Energy Institute 91 (2018) 1071–1084.

[61] G. Brenn, Droplet collision. Handbook of atomization and sprays: theory and applications, Nasser Ashgriz, 2011.

[62] N. Nikolopoulos, K.-S. Nikas, G. Bergeles, A numerical investigation of central binary collision of droplets, Computers & Fluids 38 (2009) 1191–1202.

[63] M. R. H. Nobari, J. Jan, G. Tryggvason, Head-on collision of drops - a numerical investigation, Physics of Fluids 8 (1995) 29–42.

[64] J. Li, Macroscopic Model for Head-On Binary Droplet Collisions in a Gaseous Medium, Physics Review Letters 117.

[65] M. Liu, D. Bothe, Numerical study of head-on droplet collisions at high Weber numbers, Journal of Fluid Mechanics 789 (2016) 785–805.

[66] J. Qian, C. K. Law, Regimes of coalescence and separation in droplet collision, Journal of Fluid Mechanics 331 (1997) 59–80.

[67] R. S. Volkov, G. V. Kuznetsov, P. A. Strizhak, Statistical analysis of consequences of collisions between two water droplets upon their motion in a high-temperature gas flow, Technical Physics Letters 41 (2015) 840–843.

[68] D. V. Antonov, R. S. Volkov, G. V. Kuznetsov, P. A. Strizhak, Experimental Study of the Effects of Collision of Water Droplets in a Flow of High-Temperature Gases, Journal of Engineering Physics and Thermophysics 89 (2016) 100–111.

[69] R. D. Reitz, F. V. Bracco, Mechanisms of Breakup of Round Liquid Jets, The Encyclopedia of Fluid Mechanics 3 (1986) 223–249.

[70] R. D. Reitz, Modeling atomization processes in high-pressure vaporizing sprays, Atomisation and Spray Technology 3 (1987) 309–337.

[71] P. O'Rourke, A. Amsden, The Tab Method for Numerical Calculation of Spray Droplet Breakup, SAE Technical Paper 872089 .

[72] Diesel-Egnine Management, 4th Edition, Robert Bosch GmbH, 2006.

[73] S. Budavari, The Merck index : an encyclopedia of chemicals, drugs, and biologicals, Whitehouse Station, N.J Merck, 2001.

[74] X. Jiang, A. J. James, Head-on collision of two equal-sized drops with van der Waals forces, Advances in Fluid Mechanics 37.

[75] M. Saroka, N. Ashgriz, M. Movassat, Numerical Investigation of Head-on Binary Drop Collisions in a Dynamically Inert Environment, Journal of Applied Fluid Mechanics 5 (2012) 23–37.

[76] K. G. Krishnan, E. Loth, Effects of gas and droplet characteristics on drop-drop collision outcome regimes, International Journal of Multiphase Flow 77 (2015) 171–186.

[77] Y. R. Zhang, X. Z. Jiang, K. H. Luo, Bounce regime of droplet collisions: A molecular dynamics study, Journal of Computational Science 17 (2016) 457–462.

[78] J.-P. Estrade, H. Carentz, G. Lavergne, Y. Biscos, Experimental investigation of dynamic binary collision of ethanol droplets – a model for droplet coalescence and bouncing, International Journal of Heat and Fluid Flow 20 (1999) 486–491.

[79] M. Ashna, M. H. Rahimian, LMB simulation of head-on collision of evaporating and burning droplets in coalescence regime, International Journal of Heat and Mass Transfer 109 (2017) 520–536.

[80] C. Focke, M. Kuschel, M. Sommerfeld, D. Bothe, Collision between high and low viscosity droplets: Direct Numerical Simulations and experiments, International Journal of Multiphase Flow 56 (2013) 81–92.

[81] S. Kim, D. J. Lee, C. S. Lee, Modeling of binary droplet collisions for application to inter-impingement sprays, International Journal of Multiphase Flow 35 (2009) 533–549.

[82] L. F. R. S. Rayleigh, On the instability of jets, London Mathematical Society .

[83] A. M. Worthington, A Study of Splashes, Longmans, 1908.

[84] A. Munnanur, R. D. Reitz, A new predictive model for fragmenting and non-fragmenting binary droplet collisions, International Journal of Multiphase Flow 33 (2007) 873–896.

[85] S. L. Post, J. Abraham, Modeling the outcome of drop–drop collisions in Diesel sprays, International Journal of Multiphase Flow 28 (2002) 997–1019.

[86] F. V. Bracco, Modeling of engine sprays, SAE Transactions 94 (1985) 144–167.

[87] D. L. Siebers, Liquid-phase fuel penetration in Diesel sprays, SAE Technical Paper 980809 .

[88] H. Liu, Science and Engineering of Droplets, William Andrew Inc., 1999.

[89] S. Hou, D. P. Schmidt, Adaptive collision meshing and satellite droplet formation in spray simulations, International Journal of Multiphase Flow 32 (2006) 935–956.

[90] H. Hiroyasu, M. Arai, Structures of Fuel Sprays in Diesel Engines, SAE Technical Paper 900475 .

[91] H. Hiroyasu, M. Arai, M. Tabata, Empirical Equations for the Sauter Mean Diameter of a Diesel Spray, SAE Technical Paper 890464 .

[92] H. Hiruyasu, T. Kadota, Fuel Droplet Size Distribution in Diesel Combustion Chamber, SAE Technical Paper 740715 .

[93] P. J. O'Rourke, Collective drop effects on vaporizing liquid sprays, Ph.D. thesis, Mechanical and Aerospace Engineering, Princeton University, USA .

[94] Y. Maruyama, T. Chiba, M. Saito, M. Arai, Effect of the inter-impingement system, Proceedings of ILASS-Asia (2001) 241–246.

[95] C. Arcoumanis, M. Gavaises, B. French, Effect of Fuel Injection Processes on the Structure of Diesel Sprays, SAE Technical Paper 970799 .

[96] L. Martinelli, F. V. Bracco, R. D. Reitz, Comparisons of computed and measured dense spray jets, Progress in Astronautics and Aeronautics 95 (1984) 484–512.

[97] D. R. Guilenbecher, C. López-Rivera, P. E. Sojka, Secondary atomization, Experiments in Fluids 46 (2009) 371–402.

[98] T. Kekesi, G. Amberg, L. P. Wittberg, Drop deformation and breakup, International Journal of Multiphase Flow 66 (2014) 1–10.

[99] G. Strotos, I. Malgarinos, N. Nikolopoulus, M. Gavaises, Predicting droplet deformation and breakup for moderate Weber numbers, International Journal of Multiphase Flow 85 (2016) 96–109.

[100] F. Xiao, Z. G. Wang, M. B. Sun, N. Liu, X. Yang, Simulation of drop deformation and breakup in supersonic flow, Proceedings of the Combustion Institute 36 (2017) 2417–2424.

[101] G. Strotos, I. Malgarinos, N. Nikolopoulus, M. Gavaises, Aerodynamic breakup of an n-decane droplet in a high temperature gas environment, Fuel 185 (2016) 370–380.

[102] K.-S. Im, K.-C. Lin, M.-C. Lai, M. S. Chon, Breakup modeling of a liquid jet in cross flow, International Journal of Automotive Technology 12 (2011) 489–496.

[103] M. Patterson, R. D. Reitz, Modeling the Effects of Fuel Spray Characteristics on Diesel Engine Combustion and Emission, SAE Technical Paper 980131 .

[104] L. Ricart, J. Xin, G. Bower, R. D. Reitz, In-Cylinder Measurement and Modeling of Liquid Fuel Spray Penetration in a Heavy-Duty Diesel Engine, SAE Technical Paper 971591 .

[105] J. C. Beale, R. D. Reitz, Modeling spray atomization with the Kelvin-Helmholtz/Rayleigh-Taylor hybrid model, Atomization and Sprays 9 (1999) 623–650.

[106] M. Marek, The double-mass model of drop deformation and secondary breakup, Applied Mathematical Modelling 37 (2013) 7919–7939.

[107] M. Pilch, C. A. Erdman, Use of breakup time data and velocity history data to predict the maximum size of stable fragments for acceleration-induced breakup of a liquid drop, International Journal of Multiphase Flow 13 (1987) 741–757.

[108] G. I. Taylor, The shape and acceleration of a drop in a high-speed air stream, The Scientific Papers by G. I. Taylor 3 (1963) 457–464.

[109] J. A. Nicholls, A. A. Ranger, Aerodynamic shattering of liquid drops, Journal of American Institute of Aeronautics and Astronautics 7 (1969) 285–290.

[110] E. A. Ibrahim, H. Q. Yang, A. J. Przekwas, Modeling of spray droplets deformation and breakup, Journal of American Institute of Aeronautics and Astronautics 9 (1993) 652–654.

[111] S. Som, D. E. Longman, A. I. Ramírez, S. K. Aggarwal, A comparison of injector flow and spray characteristics of biodiesel with petrodiesel, Fuel 89 (2010) 4014–4024.

[112] L. Bravo, C.-B. Kweon, A Review on Liquid Spray Models for Diesel Engine Computational Analysis, Tech. Rep., 2014.

[113] A. B. Liu, D. Mather, R. D. Reitz, Modeling the Effects of Drop Drag and Breakup on Fuel Sprays, SAE Technical Paper 930072 .

[114] D. M. Gonzalez, Z. Lian, R. D. Reitz, Modeling Diesel Engine Spray Vaporization and Combustion, SAE Technical Paper 920579 .

[115] A. B. Chhetri, K. C. Watts, Surface tensions of petro-diesel, canola, jatropha and soapnut biodiesel fuels at elevated temperatures and pressures, Fuel 104 (2013) 704–710.

[116] B. Kegl, L. Lešnik, Modeling of macroscopic mineral diesel and biodiesel spray characteristics, Fuel 222 (2018) 810–820.

[117] F. Wang, J. Wu, Z. Liu, Surface Tensions of Mixtures of Diesel Oil or Gasoline and Dimethoxymethane, Dimethyl Carbonate, or Ethanol, Energy Fuels 20 (2006) 2471–2474.

[118] T. Bohl, G. Tian, A. Smallbone, A. P. Roskilly, Macroscopic spray characteristics of next-generation bio-derived diesel fuels in comparison to mineral diesel, Applied Energy 186 (2017) 562–573.

[119] E. A. Melo-Espinosa, Y. Sánchez-Borroto, M. Errasti, R. Piloto-Rodríguez, R. Sierens, J. Roger-Riba, A. Christopher-Hansen, Surface Tension Prediction of Vegetable Oils Using Artificial Neural Networks and Multiple Linear Regression, Energy Procedia 57 (2014) 886–895.

[120] Z. Feng, C. Zhan, C. Tang, K. Yang, Z. Huang, Experimental investigation on spray and atomization characteristics of diesel/gasoline/ethanol blends in high pressure common rail injection system, Energy 112 (2016) 549–561.

[121] S. N. Sahasrabudhe, V. Rodriquez-Martinez, M. O'Meara, B. E. Farkas, Density, viscosity, and surface tension of five vegetable oils at elevated temperatures: Measurement and modeling, International Journal of Food Properties 20 (2017) 1965–1981.

[122] W. Zhao, L. Fan, Q. Dong, X. Ma, Study of Fuel Temperature Dynamic Characteristics for Diesel Engine Combination Electronic Unit Pump, Journal of Marine Science and Technology 25 (2017) 220–229.

[123] N. Ashgriz, J. Y. Poo, Coalescence and separation in binary collisions of liquid drops, Journal of Fluid Mechanics 221 (1990) 183–204.

[124] O. O. Taskiran, M. Ergeneman, Trajectory based droplet collision model for spray modeling, Fuel 115 (2014) 896–900.

[125] G. H. Ko, H. S. Ryou, Droplet collision processes in an inter-spray impingement system, Journal of Aerosol Science 36 (2005) 1300–1321.